JOURNAL OF MATERIALS SCIENCE **39** (2004) 943–949

Indentation punching through thin (011) In*P*

L. LARGEAU, G. PATRIARCHE
Laboratoire de Photonique et de Nanostructures, UPR 20 CNRS, Route de Nozay, 91460 Marcoussis, France

A. RIVIERE, J. P. RIVIERE
Laboratoire de Physique des Solides et de Cristallogénèse, UMR 8635 CNRS, 1 Pl. A. Briand, 92195 Meudon Cedex, France

E. LE BOURHIS
Université de Poitiers, Laboratoire de Métallurgie Physique, UMR 6630 CNRS, SP2MI-Téléport 2-Bd Marie et Pierre Curie, B.P. 30179, 86962 Futuroscope-Chasseneuil Cedex, France
E-mail: Eric.Lebourhis@univ-poitiers.fr

Thin (011) In*P* samples have been deformed by a Vickers indenter at 400°C under loads ranged between 0.4 N and 2.35 N. Profilometry, optical microscopy as well as scanning electron microscopy in the cathodoluminescent mode were used to get a better understanding of the plastic flow through thin samples. For the thinnest samples and highest loads, punching through the sample was detected at the opposite face. In this case, no pile up around the indent site was detected. A model describing the material flow through the samples is proposed.

1. Introduction

Plasticity of III–V semiconductors has received much attention during the past two decades because of the needs from the optoelectronic industry. Indeed, developments of heterostructures for such applications have been limited as plastic relaxation deteriously affects the performance of the devices. As a matter of fact, a better understanding of III–V semiconductors plasticity at typical temperatures used for devices elaboration (25–500°C) is required and will be of great help to improve substrate compliance and heterostructure quality [1].

As the sizes of the structures are decreasing progressively to improve integration, plasticity of finite volumes is to be understood. In this field, the indentation technique has proved to be a powerful tool to test small volume even at temperature below the brittle-ductile transition. However, contact mechanics has been developed for semi-infinite half space [2]. This assumption is not fulfilled when the size of the plastic zone becomes of the order of one of the dimensions of the object [3]. Thereafter, thin self-standing structures are expected to show a mechanical behaviour quite different from that of a bulk.

The case of (011) surfaces of III–V semiconductors is quite interesting from that point of view as plastic slip has been observed to occur in {111} planes normal to the indented surface [4, 5]. The study of the plastic response of (011) oriented samples is therefore a good test to detect difference in behaviour between thin samples and bulk samples for which a semi-infinite approximation is valid.

In this study, we have investigated the plastic behaviour of (011) In*P* at a typical process temperature (400°C). The samples were thinned progressively and indented under increasing loads. Optical, electron microscopies as well as profilometry were used to observe both sides of the samples (indented surface and bottom face) and to detect changes in material flow due to the finite thickness of the samples.

2. Experimental procedures

2.1. Material and sample preparation

We used Czochalski grown single crystals of (011) In*P* which were not intentionally doped ($n \sim 10^{16}$ cm^{-3} Hall effect measurement). One of the faces was epiready, the other one was mechanically and chemically polished using a 1% bromine-methanol solution to prepare 4 sets of samples of thickness ranged between 170 and 350 μm (Table I).

2.2. Deformation of the sample

The samples were deformed by a Vickers diamond pyramid at 400°C in air atmosphere. All sets of samples were indented using 5 different loads ranged between 0.4 and 2.35 N (Table I). For each load the indentation test was repeated twice. The samples were set on a home-designed holder in which a 1.3 mm-wide trench was machined so that the bottom face of the sample underneath the indent site was not in contact with the holder. The indenter was left 60 s on the sample before being raised up. On each samples, arrays of indentations (aligned along the trench) were made for subsequent detection in the microscopes and in the surface profiler. One side of the indentation was aligned along

TABLE I Samples thickness and indentation loads used for this study. Indentation tests were repeated twice under each load. The number (0, 1 or 2) when a deformation of the bottom face was observed is reported for all the 20 different conditions

Sample thickness (μm) Indentation load (N)	170	200	250	350
0.4	0	0	0	0
0.9	2	0	0	0
1.35	2	2	0	0
1.9	2	2	1	0
2.35	2	2	2	0

the [0$\bar{1}$1] direction, the other one being aligned along the [100] orthogonal direction.

2.3. Sample observations

When the indentation tests were completed, the samples were cooled down to room temperature (RT) and observations of the two faces (front and bottom) were made by interferential optical microscopy (IOM) in the Nomarsky mode. Profile measurements were performed to obtain quantitative results on the surface topography of the indented and bottom sides. A scanning electron microscope (Jeol JSM 840) was operated in the cathodoluminescent mode (CL) to observe both sides of the sample using a S20R detector.

3. Results

3.1. Comparison of the topography of the indented surface of thinnest and thickest samples

Fig. 1 shows the height profiles of indents made under the same load (2.35 N, e.g., maximum load used here) in both samples (170 and 350 μm thick). The profiles were captured along the same [100] direction and approximately through the indent site centre.

The profile corresponding to the thickest sample reveals pile up around the indentation (Fig. 1a). These pile-ups have extensions about twice the indentation width and reveal plastic deformation of the surface at large distances from the indent site. Such pile-ups are commonly observed in (001) bulk In*P* indented at the same temperature [6].

In contrast, no pile-up could be detected at the indented surface of the thinnest samples (170 μm) under the same load (2.35 N, Fig. 1b). This is a very interesting result since it reveals that indentation plasticity around the indent site is modified when the sample thickness is reduced. As discussed in more details below, these changes observed at the indented surface are to be related to the emergence of the plastic flow at the bottom surface.

3.2. Observation of the front and bottom surfaces of the samples

Fig. 2 shows the front and back sides of the 170 μm thinnest sample deformed under two different loads (0.9 and 1.35 N). The front face shows the typical Vickers mark which size increases with increasing load. Al-

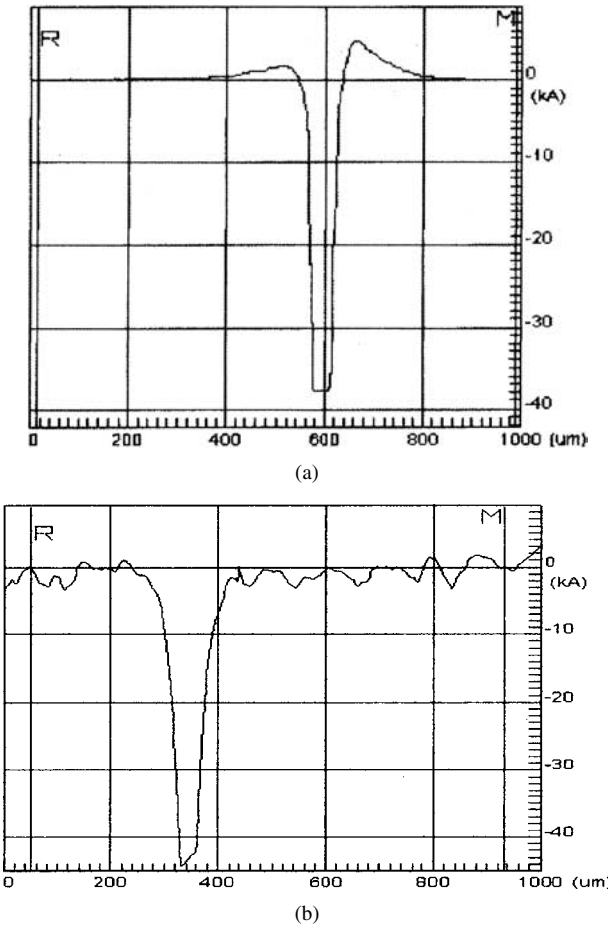

Figure 1 Height profiles along [100] of the indented surface of (011) In*P* deformed under 2.35 N at 400°C. The thickness of the sample is respectively (a) 350 μm and (b) 170 μm. Pile up is observed on the thickest sample while this phenomenon is not detected in the thinnest one. The Vickers profile is to be considered with care since it is very difficult to scan through the indent centre and as a cut off of the scale is introduced by the profiler. Undulation of the surface in (b) is due to the polishing of the sample (Section 2).

most no radial cracking is observed for an indentation temperature of 400°C in contrast to RT experiments where brittle fracture was observed to propagate in dislocation-free zones under similar loads (0.2–1 N) [5].

The back side shows characteristic slip lines that were observed in a diamond-shaped area (Fig. 2d). Such slip lines correspond to the plastic deformation of the back surface at the bottom of the indent site. The diamond-shaped area was observed to be much larger than the Vickers mark generated at the indented surface. The latter corresponds to the area that was in contact with the indenter while plastic deformation is revealed in an area much larger at the bottom surface. The slip lines were observed to align along the ⟨211⟩ directions parallel to the indented surface. These directions form an angle of approximately 70° and correspond to the intersection between the bottom face and the {111} slip planes normal to the indented surface.

Under 0.9 N, it is more difficult however to detect slip lines using only IOM (Fig. 2b). Fig. 3a shows a CL image of the back face of the 170 μm thick sample indented under 0.9 N that is to be compared to the IOM micrograph of Fig. 2b. The CL image allows to reveal

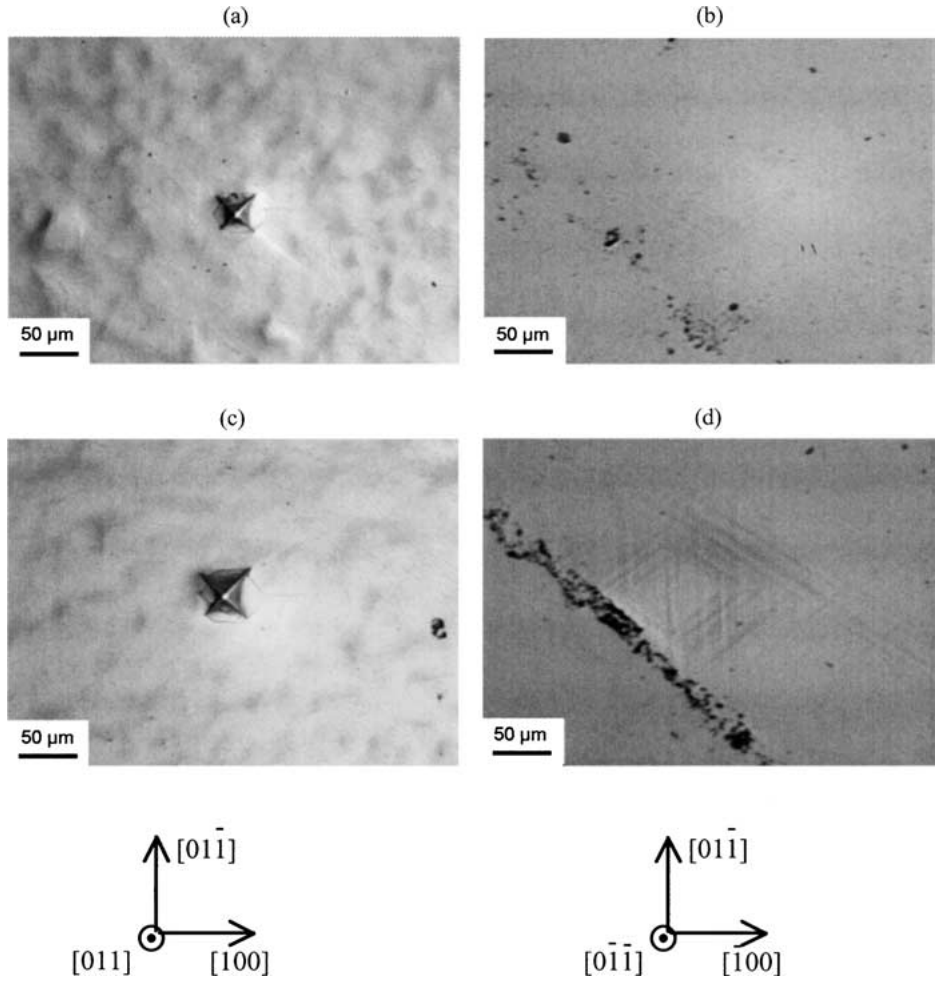

Figure 2 Optical micrographs of the top surface (a–c) and bottom surface (b–d) of a 170 μm thick (011) InP indented at 400°C under (a–b) 0.9 N and (c–d) 1.35 N. The deformation of the bottom surface is hardly detectable under 0.9 N (c) while slip lines are clearly observed under 1.35 N (d). In (d) the dark line corresponds to contamination of the sample while transferring from the indentation machine.

without ambiguity plastic flow at the bottom surface as dark-contrasted lines arranged in a diamond-shaped area can be observed. In fact, the CL technique allows to detect with good contrast non-radiative defects like dislocations in semiconductors [7].

Interestingly, in the case of the 350 μm thickest samples, observation of the bottom surface never revealed deformation of the back side even when CL was used. Table I summarizes the observations of the bottom face for all the samples. Indentation tests were repeated twice under each load. The number (0, 1 or 2) when a deformation of the bottom face was observed is reported for all the 20 different conditions. For intermediate thickness of the samples (200 and 250 μm) deformation of the back side could be observed although under higher loads than for the 170 μm thick sample. It is concluded that plastic deformation of the back side of the sample occurs when a compromise between the indentation load and the sample thickness is met. In such case plastic slip lines are detected in a diamond-shaped area and are indicative of plastic flow in {111} slip planes normal to the indented surface. It is worth noting however that the CL micrographs (see for example Fig. 3b, obtained for a test under a 1.9 N load for a sample thickness 170 μm) reveal a few dislocations outside the diamond-shaped area described above which origin will be discussed below.

3.3. Topography of the bottom face

To get more quantitative results on the material punching through the sample, profiles of the bottom surfaces were captured. For example, Fig. 4 shows profiles obtained under a load of 2.35 N in the case of the 170 μm thick sample. The height of the deformed zone at the bottom surface is determined to be only 1.5 μm under 2.35 N. Indeed, such small difference in height is hardly detectable by IOM.

Two profiles have been made systematically, one along the [$\bar{1}$00] direction and another one along the orthogonal [01$\bar{1}$] direction. The profiles show different width as expected from the IOM and CL observations which revealed a diamond-shaped deformed zone at the back surface. To determine the sizes of the diamond-shaped area, the profiles were fitted by linear sides. The intercepts of such triangular profiles with the x-axis allowed to determine the widths W_{100} along [100] and $W_{0\bar{1}1}$ along [0$\bar{1}$1]. Under 2.35 N, these widths are determined to be 231 and 157 μm respectively (Fig. 4). These values are about 150 and 100 times the height of deformed zone and are indicative of a very smooth topography. Furthermore, the aspect ratio $W_{100}/W_{0\bar{1}1}$ can be determined to be about 1.42 in good agreement with expected angles between slip planes. Nonetheless, some discrepancy between both values is expected and is to be attributed to the complex tails of the profiles

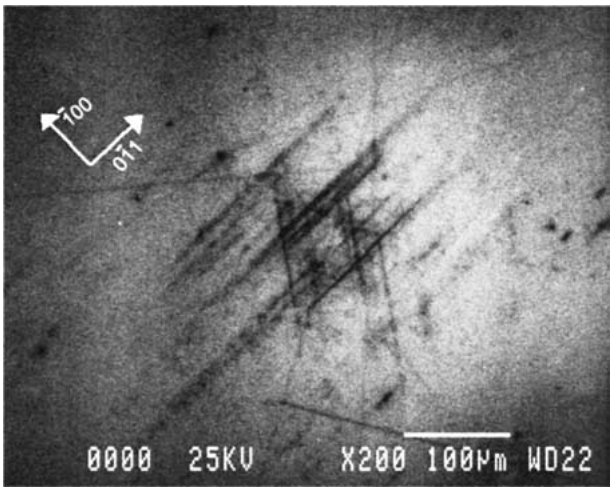

(a)

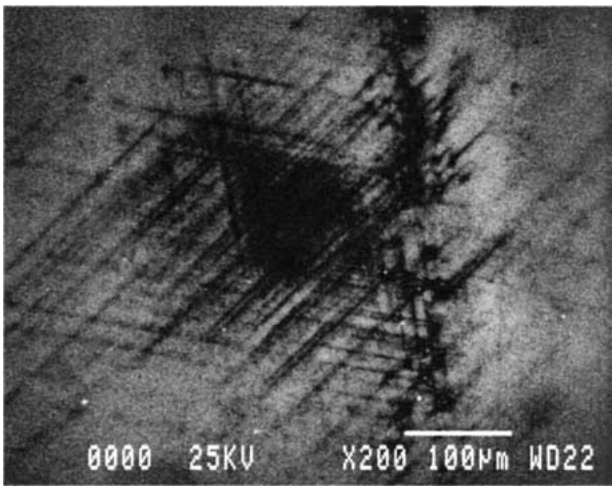

(b)

Figure 3 CL micrograph of the bottom surface of a 170 μm thick (011) InP indented at 400°C under (a) 0.9 N and (b) 1.9 N. CL allows detecting plastic flow at the bottom surface unambiguously under 0.9 N (compare Figs 3a and 2b).

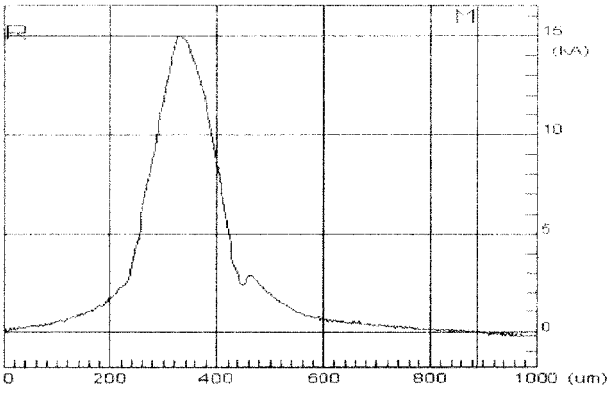

(a)

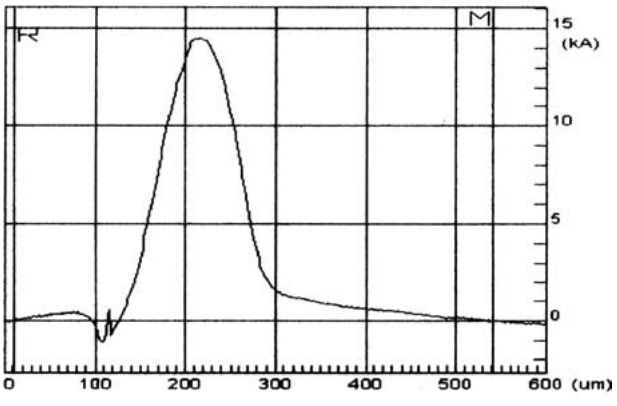

(b)

Figure 4 Height profiles of the bottom surface of the 170 μm thick (011) InP indented at 400°C under 2.35 N. The profiles were captured along (a) [100] (b) [0$\bar{1}$1].

and also to the uncertainty to capture a scan through the diamond-shaped area centre.

It is concluded that plastic deformation of the back surface is detected in a diamond shaped area which sizes are about twice the diagonal of the Vickers marks (about $D = 78\ \mu$m under 2.35 N for the 170 μm thick sample). Therefore, profilometry confirms that the volume of a thin sample that is plastically deformed has a size that is much larger than the size of the area that was in contact with the indenter. It is well known that indentation of a semi-infinite half space generates a plastic zone which radius ranges between two or three times the contact radius [2]. Our results show that punching of a thin sample affects also a large volume as its lateral size is about twice larger than the contact area dimension.

3.4. Material 'transfer' from the indented surface to the bottom face

Firstly, we determined the volume of the material that was punched out of the sample (at the back side). We assumed that this volume can be approximated by a pyramid with a diamond-shaped base which sizes were determined by profilometry and are W_{100} along [100] and $W_{0\bar{1}1}$ along [0$\bar{1}$1] as detailed in Section 3.3. Therefore, the volume V_b of such a pyramid is given by

$$V_b = 1/6 \cdot W_{100} \cdot W_{0\bar{1}1} \cdot h \quad (1)$$

where h is the height of the deformed volume.

We compared this volume V_b to the volume V_i of the material punched into the sample by the indenter. This volume is that of the Vickers mark which is a function of the mean diagonal size D and the residual depth h_r of the indentation:

$$V_i = 1/6\, D^2 \cdot h_r \quad (2)$$

In the following, we neglected the elastic recovery of the Vickers mark [8, 9] and took for h_r the contact depth value h_c that is geometrically determined as

$$h_c = D/7 \quad (3)$$

Combining Equations 1–3 let V_b/V_i be

$$V_b/V_i = 7 \cdot (W_{100} \cdot W_{0\bar{1}1} \cdot h)/(D^3) \quad (4)$$

V_b/V_i ratio can be considered as a measure of the 'material transfer' from the indented surface to the back side of the sample. Fig. 5 plots V_b/V_i ratio for the 170 μm thick sample. V_b/V_i ratio is zero for loads less

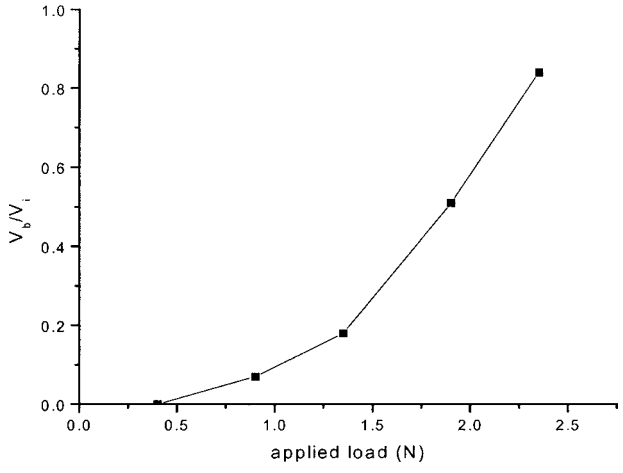

Figure 5 V_b/V_i ratio as a function of applied load for the 170 μm thick (011) InP indented at 400°C. V_b is the volume of the plastically deformed zone at the bottom of the sample while V_i is the volume of the Vickers indentation (refer to Equations 1–4).

than 0.4 N, indeed no material flow could be detected at the bottom surface under such indenting loads even using CL (Table I). From 0.9 N and above, V_b/V_i ratio increases progressively to reach almost 84% under a load of 2.35 N. This latter value shows that the 'material transfer' from the indented surface to the back surface of the sample under the highest loads is very effective under such experimental conditions.

4. Discussion

4.1. Limits of the semi-infinite half space description

As described above plastic deformation of the back side of the sample in {111} normal slip planes could be detected for the thinnest sample under a 0.9 N load and above. Further, when a back side deformation was detected, no pile up was observed around the indent site (Fig. 1b). Both results are to be correlated. Pile up appears for thick samples where no material flow through the sample is allowed. Therefore, the finite thickness of the samples may have a great influence on the response to contact loading.

Indentation mechanics developed for semi-infinite half space allows to determine the plastic-zone radius c to be about 2–3 times the half of the diagonal $c \sim (2–3) \cdot D/2$ [2, 10, 11]. Under a load of 0.9 N, the diagonal is $D = 45$ μm for the 170 μm thick sample so that the radius of the plastic zone in a semi-infinite sample would be ranged between 90 and 135 μm respectively. These plastic-zone extensions are of the same magnitude as one of the dimensions of the sample (here the thickness $e = 170$ μm). Indeed c/e is determined to be 0.5 and 0.8 respectively. Therefore, it can be concluded that when c/e reaches 50% (c from infinite half space indentation mechanics), drastic changes in the material flow will happen as revealed here in InP around the indent site as well as at the opposite surface.

A commonly accepted guideline suggests the use of an indent depth <10% of the layer thickness to determine the property of a thin layer [12]. Indeed, we have shown here that when h_c/e approaches 3.7% (h_c from Equation 3) the sample cannot be considered as a semi-infinite half space any more.

4.2. Punching mechanism

The slip lines forming the diamond-shaped area observed at the bottom surface of the thinnest sample are the signatures of plasticity in {111} slip planes normal to the indented surface. These slip planes were observed to operate also in bulk samples [5]. Such plasticity can be described by the generation and development of dislocation loops in the {111} slip planes normal to the indented surface as schematised in Fig. 6. The Vickers mark is drawn in the diamond-shaped area formed by the emergence of the {111} slip planes normal to the indented surface. As observed by IOM and CL, the sides of this area are parallel to the ⟨211⟩ directions, which form a 70° angle.

It should be noted that Fig. 6 scheme cannot describe all the indentation process. Indeed, observation of the bottom surface showed plasticity at distances over two to three times the indent mark size, which Fig. 6 does not describe. Furthermore, the punching of the indent is a violent phenomenon and the mark of the Vickers pyramid is generated without consideration of crystallography except for some particular cases at the end of the indentation process [6]. If we consider only the gliding in the vertical {111} planes schematised in Fig. 6, the mark of the indenter would not be Vickers but diamond shaped. Nonetheless, indentation process leads to the gliding drawn in vertical slip planes revealed experimentally and schematised in Fig. 6.

In Fig. 6, two dislocations with identical Burgers vector $b = [0\bar{1}\bar{1}]$ have been drawn. The development of the loops and their interaction lead to the annihilation

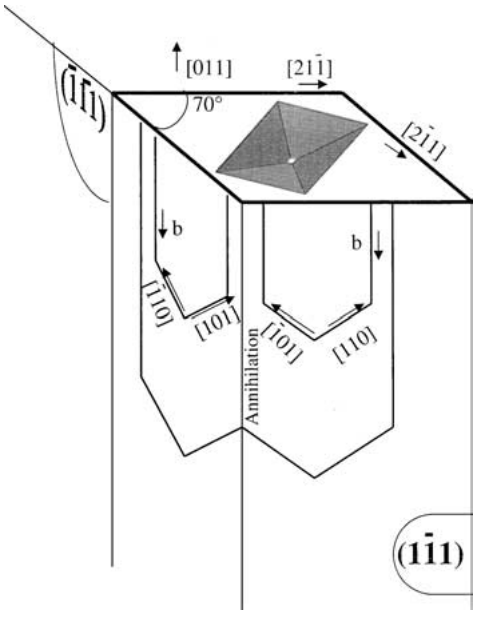

Figure 6 Schematic representation of the punching. Gliding in {111} planes normal to the (011) indented surface is described. Two dislocations loops with the same Burgers vector **b** are assumed to be nucleated and develop in their respective slip planes. Annihilation of the screw segments along the intersection of the $(\bar{1}\bar{1}1)$ and $(1\bar{1}1)$ leads in a second step to a half loop.

of two screw segments. Deviation or annihilation of the other screw segments lead to the gliding of prismatic loops through the sample. It should be noted that dislocation extension along the ⟨211⟩ directions outside the diamond-shaped area may happen as revealed by CL (Fig. 3). Further, using CL, some slip traces could be observed along $[01\bar{1}]$ and correspond to plastic deformation in {111} slip planes inclined to the indented surface that may also operate [4, 5]. Nonetheless, the IOM and CL observations of the bottom side showed that most of slip lines are parallel to ⟨211⟩ directions and arranged in a diamond-shaped zone. Therefore, we can assume that the punching mechanism proposed in Fig. 6 is representative of the main plastic flow through thin samples.

4.3. Punching arrest

The punching mechanism described in Fig. 6 is to be reiterated as long as the indentor stresses overbalance the material resistance to plastic deformation. As described above the material flow has been observed to occur mainly in {111} slip planes normal to the indented surface. Once the material flow reaches the opposite surface, the volume of the material that is plastically deformed has the diamond-shaped projection observed in Fig. 2. Let us define the elastic-plastic boundary as the surface separating the elastic and plastic domains [2]. For a semi-infinite half space, the elastic-plastic boundary is almost hemispherical (expanding cavity model [2, 10, 11]). In the case of a sample with finite depth, once the material flow has reached the surface opposite to the indented surface, expansion of the plastic zone is only lateral as one dimension is fixed to the thickness of the sample.

Once punching through the sample begins, we shall assume a pure shear stress field at the elastic-plastic boundary. An increase of the load ΔF applied to the indenter yields an increase ΔS of the lateral surface of the elastic-plastic boundary:

$$\Delta F = \Delta S \cdot \tau_o \tag{5}$$

where τ_o is the material friction. The surface S of the elastic-plastic boundary is a function of the sizes W_{100} and $W_{0\bar{1}1}$ of the diamond shaped area and the thickness e of the sample:

$$S = \sqrt{\left(W_{100}^2 + W_{0\bar{1}1}^2\right)} \cdot e = P \cdot e \tag{6}$$

where we define P as the perimeter of the elastic-plastic boundary.

From Equations 5 and 6 an increment ΔF of the load applied on the indenter leads to an increase $\Delta P = \Delta S/e$ of the perimeter of the elastic-plastic boundary. Fig. 7 plots the elastic-plastic boundary perimeter as a function of the load applied on the indenter for the 170 μm thick sample (zero value means that no back side deformation was detected cf Table I). It should be noted that the model presented above is to be used only when full punching through the sample is achieved. In that case, a linear dependence of P with F should be observed following Equation 5. A linear fit of the experimental data (for $F \geq 0.9$ N) has been determined and is shown in Fig. 7. It allows to determine τ_o to be about 50 MPa. This value is usefully compared to the critical resolved shear stress (CRSS) values which are usually determined from stress-strain compression curves. CRSS values generally show a strong dependence on temperature and strain rate. Indeed for an undoped material a CRSS value of 14 MPa is reported at 350°C for a strain rate of $\bar{\varepsilon} = 10^{-4}$ s^{-1} [13] while CRSS values about 26 and 12.5 MPa are reported at 290 and 390°C respectively for $\bar{\varepsilon} = 10^{-5}$ s^{-1} [14]. The material friction τ_o determined here has the same magnitude as the CRSS mentioned above. Discrepancy is expected however as our determination is dependent on our ability to localise the elastic-plastic boundary and because of

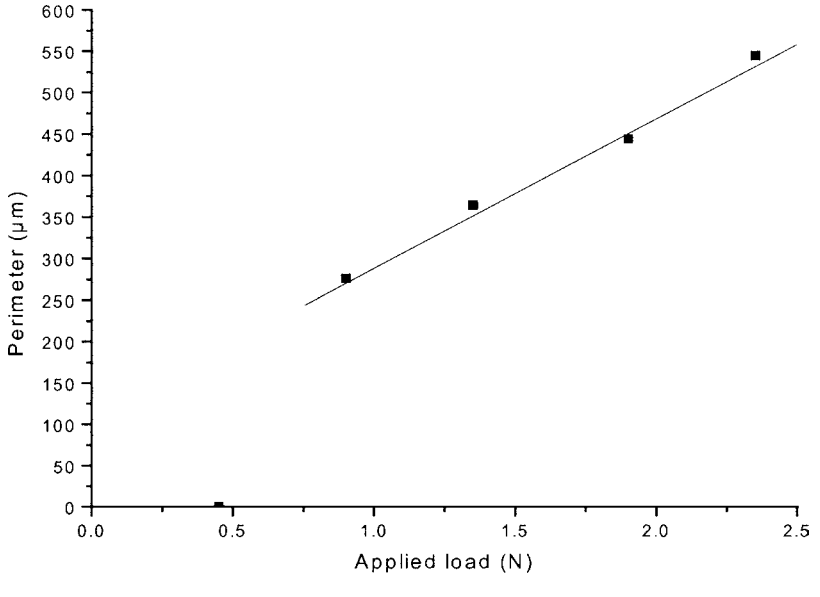

Figure 7 Perimeter P of the elastic-plastic boundary as a function of applied load F in the 170 μm thick (011) InP sample indented at 400°C. See definition of P in the text (Sections 3.3 and 4.2, Equations 3 and 4). The linear fit of P versus F is shown for loads over 0.9 N. In this range of loads deformation of the back side was observed.

the assumptions used to model the plastic punching. Moreover, a thermal gradient is expected in the sample as a cooling of the surface ($\Delta T \sim 10^{\circ}$C) was observed during the test when the diamond pyramid was in contact with the sample. Therefore, crystal friction $\tau_o(z)$ is a function of the depth z with $\tau_o(0) > \tau_o(e)$ while we considered an average value over the depth.

5. Conclusion

The study of indentations made in thin (011) InP has revealed that contact behaviour is changed when one of the dimensions of the object (here the thickness) is of the same magnitude as the plastic zone dimension. Indeed, we have observed that when the thickness of the sample is progressively reduced and the indentation load increased, punching through the thin samples may occur. In such case, pile up is not detected any more around the indent site. Thereafter, the infinite half space asumption commonly used in indentation mechanics needs to be reconsidered, as it is not fulfilled. A model for plastic punching has been proposed for the (011) oriented surface that was investigated here. Nonetheless, it would be important to test other surfaces like (001) and (111) where plastic deformation has been reported to occur in inclined slip planes. Therefore, geometrical factors are to be taken into consideration in those cases [4, 6]. Furthermore, Johnson's cavity model allows predicting the plastic zone radius to be inversely proportional to the square root of the yield stress [1–3, 15, 16]. Subsequent, II–VI semiconductors are expected to show deviations to semi-infinite indentation mechanics under lower loads and/or lower temperature. The paper also proposes a new method to determine crystal friction of small volumes. Noticeably, at intermediate temperature brittle fracture may occur and the adjustment of the thickness of the foil is to be optimised. In future work, we shall determine hence the change in crystal friction with temperature. The technique might also be of great help in the future as miniaturisation is required by the optoelectronic industry. Further, the method allows to get information at elevated temperature used for device fabrication.

References

1. G. PATRIARCHE and E. LE BOURHIS, *Appl. Surf. Sci.* **178** (2001) 134.
2. K. L. JOHNSON, "Contact Mechanics" (Cambridge University Press, 1985).
3. Y. CHOI and S. SURESH, *Scripta Mater.* **48** (2003) 249.
4. X. J. NING, T. PEREZ and P. PIROUZ, *Phil. Mag.* A **72** (1995) 837.
5. E. LE BOURHIS, G. PATRIARCHE, L. LARGEAU and J. P. RIVIERE, *J. Mater. Sci. Lett.* **20** (2001) 1361.
6. E. LE BOURHIS, J. P. RIVIERE and A. ZOZIME, *J. Mater. Sci.* **31** (1996) 6571.
7. B. G. YACOBI and D. B. HOLT, *J. Appl. Phys.* **59** (1986) R1.
8. W. C. OLIVER and G. M. PHARR, *J. Mater. Res.* **7** (1992) 1564.
9. T. SUZUKI and T. OHMURA, *Phil. Mag.* A **74** (1996) 1073.
10. L. E. SAMUELS and T. O. MULHEARN, *J. Mech. Phys. Sol.* **5** (1957) 125.
11. M. M. CHAUDHRI, *Acta Mater.* **46** (1998) 3047.
12. A. K. BHATTACHARYA and W. D. NIX, *Int. J. Sol. Struct.* **24** (1986) 1287.
13. P. GALL, J. P. PEYRADE, R. COQUILLE and F. REYNAUD, *J. Cryst. Growth* **82** (1987) 689.
14. E. LE BOURHIS, A. ZOZIME, A. RIVIERE and C. VERMEULIN, *J. Phys. III.* **5** (1995) 1795.
15. D. KRAMER, H. HUANG, M. KRIESE, J. ROBACH, J. NELSON, A. WRIGHT, D. BAHR and W. W. GERBERICH, *Acta Mater.* **47** (1998) 333.
16. Y. L. CHIU and A. H. W. NGAN, *ibid.* **50** (2002) 2677.

Received 28 February
and accepted 16 September 2003